Int. J. Solids Structures, 1968, Vol. 4, pp. 421 to 446. Pergamon Press. Printed in Great Britain

THE BUCKLING AND POST-BUCKLING BEHAVIOR OF SPHERICAL CAPS UNDER CONCENTRATED LOAD*

JAMES R. FITCH†

Harvard University, Cambridge, Massachusetts

Abstract—The elastic buckling and initial post-buckling behavior of clamped shallow spherical shells under concentrated load is considered. It is found that bifurcation into an asymmetric deflection pattern will occur before axisymmetric snap-buckling unless the ratio of the shell rise to the thickness lies within a narrow range corresponding to relatively thick shells. The initial post-buckling analysis indicates that the shell retains its load carrying capacity as it makes the transition to asymmetric behavior. These results are in qualitative agreement with available experimental data.

INTRODUCTION

THE subject of this paper is the buckling and post-buckling behavior of clamped spherical caps loaded by an inwardly directed concentrated force at the apex (Fig. 1). Several previous

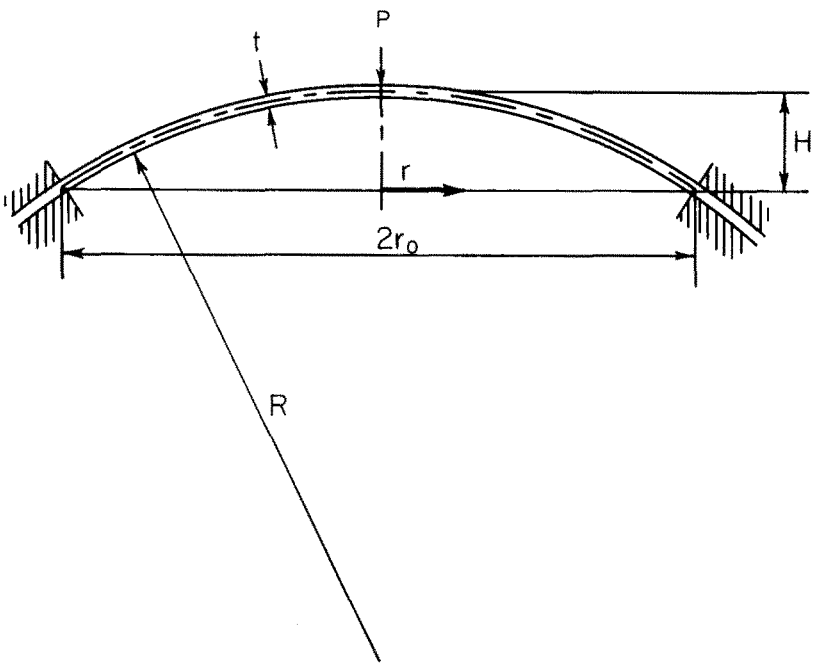

FIG. 1. Geometry of a clamped spherical cap.

* This work was supported in part by the National Aeronautics and Space Administration under Grant NsG-559, and by the Division of Engineering and Applied Physics, Harvard University.

† Now at: Knolls Atomic Power Laboratory, General Electric Company, Schenectady, N.Y. 12301.

studies of this problem [1–6] have dealt with the question of finding the critical load for axisymmetric snap-buckling. The work presented here was undertaken to investigate the possibility that the deformation of the cap becomes asymmetric at a load below the critical load predicted by the axisymmetric theory. The locus of equilibrium points on a plot of load vs. apex deflection might, for example, have a bifurcation point as shown in Fig. 2.

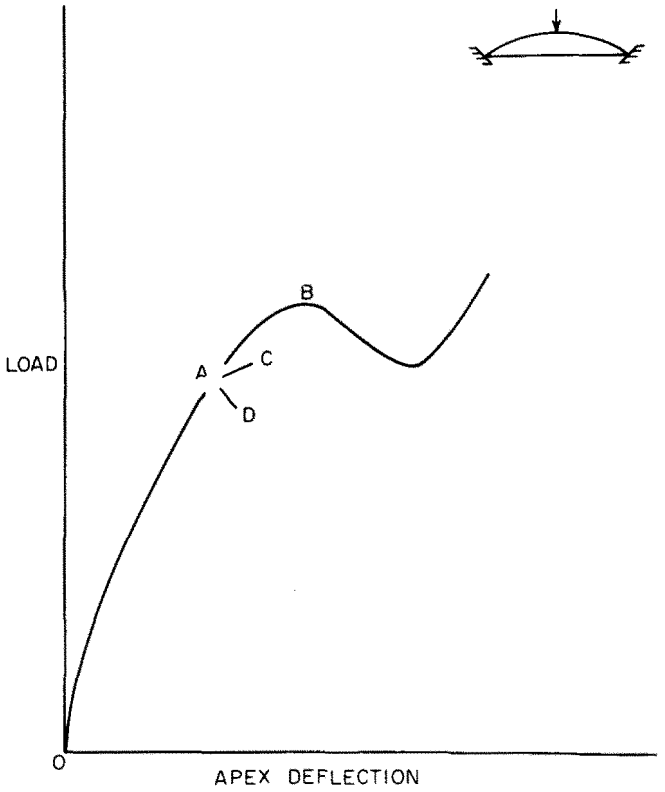

FIG. 2. Hypothetical load–deflection curve for a clamped spherical cap.

On this plot the fundamental axisymmetric equilibrium path is represented by OAB. The load corresponding to the local maximum at B is the critical load for axisymmetric snap-buckling. Asymmetric deformation could, however, start to develop at the smaller load corresponding to the bifurcation point A. In the neighborhood of A the bifurcation path could initially rise or fall. A rising curve (AC) means that the transition to asymmetric behavior occurs smoothly without loss of load-carrying capacity. A falling curve (AD), on the other hand, indicates that the transition is marked by sharp snap-buckling. The objective of the present study, then, is the calculation of the minimum load at which asymmetric bifurcation can occur, and the initial slope of the bifurcation path.

The axisymmetric studies referred to above date back to the work of Biezeno [1]. In his analysis, as well as in that of Chien [2] and Ashwell [3], an approximate technique was used to account for the non-linear character of the problem. The critical loads predicted by these authors for a cap without edge moment or horizontal restraint are in reasonable agreement

with each other, and with experimental values obtained by Ashwell. Archer [4] carried out the first detailed numerical study of the unrestrained edge problem. He used a direct iterative technique to solve Reissner's non-linear equations, and calculated the load deflection curve up to the point at which the procedure first failed to converge. He hypothesized that the convergence failure was caused by the fact that a local maximum had been reached, and he presented the corresponding load as the critical load. In making this hypothesis he recognized the possibility that the convergence failure might have occurred at a load significantly below the true maximum. Mescall [5, 6] used a different numerical technique to solve the same equations and found that, except for relatively thick shells, the true maximum did occur well beyond the point where Archer's procedure failed to converge. His results agreed well with experimental critical loads reported by Evan–Iwanowski [7]. He also calculated load–deflection curves possessing a local maximum for the clamped cap. Penning and Thurston [8] undertook a joint analytical and experimental study of the clamped cap. Their experiments indicate that the deflection will become asymmetric before axisymmetric snap-buckling occurs. Their data also indicate that the shell retains its load-carrying capacity as it makes the transition to asymmetric behavior. The analytical and numerical work reported by these authors, however, failed to predict the existence of critical loads for asymmetric buckling.

In this paper a detailed investigation of the clamped edge problem is carried out on the basis of Marguerre's non-linear shallow shell theory [9]. Critical loads for asymmetric buckling are calculated by a standard perturbation technique which leads to a linear eigenvalue problem. Then an extension of the perturbation idea is used to investigate the initial post-buckling behavior, and in particular to calculate the initial slope of the bifurcation equilibrium path.

The results of the present buckling calculation were shown previously in a survey paper by Budiansky and Hutchinson [10]. Also, through a recent personal communication the author was made aware of a study of the buckling problem by Bushnell [11] of the Lockheed Palo Alto Research Laboratory. The numerical results obtained by him are in excellent agreement with those of the present study.

BUCKLING OF A SPHERICAL CAP

Basic equations

The analysis will be restricted to shells which are both thin and shallow. This means that the ratio of the thickness to the radius of curvature is much less than unity, and that the ratio of the apex rise to the base diameter is less than about $\frac{1}{8}$. With these restrictions Marguerre's non-linear shallow shell equations can be used. For a spherical cap under concentrated load these equations can be written in the non-dimensional form

$$\nabla^4 w = \nabla^2 f + \left(\frac{1}{x} f' + \frac{1}{x^2} \dot{f}\right) w'' + \left(\frac{1}{x} w' + \frac{1}{x^2} \dot{w}\right) f'' - 2\left(\frac{1}{x} \dot{f}' - \frac{1}{x^2} \dot{f}\right)\left(\frac{1}{x} \dot{w}' - \frac{1}{x^2} \dot{w}\right) + \frac{2p\delta(x)}{x} \tag{1}$$

$$\nabla^4 f = -\nabla^2 w + \left(\frac{1}{x} \dot{w}' - \frac{1}{x^2} \dot{w}\right)^2 - \left(\frac{1}{x} w' + \frac{1}{x^2} \dot{w}\right) w'' \tag{2}$$

where x and θ are polar coordinates in the base plane (Fig. 3) and

$$()' \equiv \frac{\partial}{\partial x}(); \qquad \dot{()} \equiv \frac{\partial}{\partial \theta}()$$

$$\nabla^2() = ()'' + \frac{1}{x}()' + \frac{1}{x^2}(\ddot{}) .$$

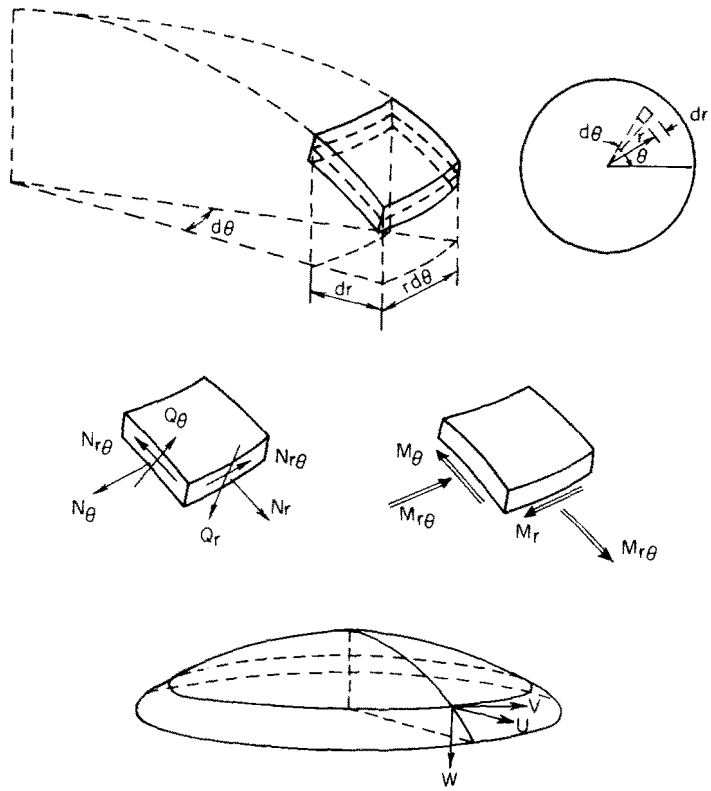

FIG. 3. Stress resultants, moments, and displacements.

The symbol $\delta(x)$ denotes the standard "delta-function" which has the properties

$$\delta(x) = 0 \qquad x \neq 0$$

$$\int_0^x \delta(y)\,dy = \tfrac{1}{2} \qquad x > 0.$$

The non-dimensional radial coordinate x, vertical deflection w, stress function f, and load p are related to the corresponding dimensional quantities by

$$x = \frac{\lambda}{r_0} r \qquad w = \frac{\lambda^2}{2H} W$$

$$f = \frac{\lambda^4}{4EH^2 t} F \qquad p = \frac{PR}{2\pi D}$$

where r_0, H, t, and R are respectively the base radius, apex rise, thickness, and radius of curvature of the shell (Fig. 1), E is Young's modulus, and D is the bending stiffness $[= Et^3/12(1-\nu^2)]$. The geometry parameter λ is defined by

$$\lambda = 2[3(1-\nu^2)]^{1/4}\left(\frac{H}{t}\right)^{1/2}$$

and ν is Poisson's ratio. A similar non-dimensionalization was introduced by Huang [12] in his treatment of the spherical cap under uniform pressure. The completely clamped condition at the outer edge (no displacement or rotation) means that for $x = \lambda$

$$w = 0 \tag{3}$$

$$w' = 0 \tag{4}$$

$$f'' - \frac{\nu}{\lambda} f' - \frac{\nu}{\lambda^2} \dot{f} = 0 \tag{5}$$

$$\lambda\left(f'' - \frac{\nu}{x} f' - \frac{\nu}{x^2} \dot{f}\right)' - \frac{1}{\lambda} f' - \frac{1}{\lambda^2} \dot{f} + \nu f'' + 2(1+\nu)\left(\frac{1}{x} \dot{f}\right)' = 0 . \tag{6}$$

Huang has shown that (5) and (6) are equivalent to the statement that the horizontal radial and horizontal tangential displacements vanish at the boundary. Equations (1)–(6), when augmented by appropriate conditions at the apex, give a complete description of the problem.

Axisymmetric behavior

If the deformation is axisymmetric it is easily shown that the above equations reduce to

$$(x\Theta')' - \frac{1}{x}\Theta + x\Phi = -p + \Theta\Phi \tag{7}$$

$$(x\Phi')' - \frac{1}{x}\Phi - x\Theta = -\tfrac{1}{2}\Theta^2 \tag{8}$$

$$\Theta(\lambda) = 0 \tag{9}$$

$$\lambda\Phi'(\lambda) - \nu\Phi(\lambda) = 0 \tag{10}$$

where $\Theta = -w'$ and $\Phi = f'$. The description of the axisymmetric problem can be completed by requiring that the shell remain smooth at the apex, and that the membrane forces remain bounded. These conditions cannot be satisfied unless

$$\lim_{x \to 0} \Theta, \Phi = 0 . \tag{11}$$

Equations (7)–(11) have been obtained by several previous investigators [4, 5, 8]. They govern the cap behavior until asymmetric bifurcation occurs.

Buckling equations

To detect the occurrence of bifurcation buckling a solution to (1)–(6) is sought in the form

$$\begin{Bmatrix} w \\ f \end{Bmatrix} = \begin{Bmatrix} \int_x^\lambda \Theta \, dx \\ \int_0^x \Phi \, dx \end{Bmatrix} + \xi \begin{Bmatrix} w_1(x,\theta) \\ f_1(x,\theta) \end{Bmatrix} \tag{12}$$

where ξ is an infinitesimal scalar parameter. Substitution of (12) in (1)–(6), simplification with the help of (7)–(11), and linearization with respect to ξ gives

$$\nabla^4 w_1 = \nabla^2 f_1 - \left(\frac{1}{x} f'_1 + \frac{1}{x^2} \ddot{f}_1\right)\Theta' + \frac{1}{x} w''_1 \Phi$$
$$- \frac{1}{x} f''_1 \Theta + \left(\frac{1}{x} w'_1 + \frac{1}{x^2} \ddot{w}_1\right)\Phi'$$
$$\nabla^4 f_1 = -\nabla^2 w_1 + \left(\frac{1}{x} w'_1 + \frac{1}{x^2} \ddot{w}_1\right)\Theta' + \frac{1}{x} w''_1 \Theta$$

and boundary conditions (3)–(6) on (w_1, f_1). The buckling equations constitute a linear eigenvalue problem in which the parameter p, whose lowest eigenvalue is sought, enters implicitly through the functions Θ and Φ. If the solution is taken in the form

$$\begin{Bmatrix} w_1 \\ f_1 \end{Bmatrix} = \begin{Bmatrix} w_{1n} \\ f_{1n} \end{Bmatrix} \cos n\theta$$

the equations for (w_{1n}, f_{1n}) are found to be

$$L_n^2(w_{1n}) = L_n(f_{1n}) - \left(\frac{1}{x} f'_{1n} - \frac{n^2}{x^2} f_{1n}\right)\Theta' + \frac{1}{x} w''_{1n}\Phi - \frac{1}{x} f''_{1n}\Theta + \left(\frac{1}{x} w'_{1n} - \frac{n^2}{x^2} w_{1n}\right)\Phi' \tag{13}$$

$$L_n^2(f_{1n}) = -L_n(w_{1n}) + \left(\frac{1}{x} w'_{1n} - \frac{n^2}{x^2} w_{1n}\right)\Theta' + \frac{1}{x} w''_{1n}\Theta \tag{14}$$

$$w_{1n}(\lambda) = 0 \tag{15}$$

$$w'_{1n}(\lambda) = 0 \tag{16}$$

$$f''_{1n}(\lambda) - \frac{\nu}{\lambda} f'_{1n}(\lambda) + \frac{n^2 \nu}{\lambda^2} f_{1n}(\lambda) = 0 \tag{17}$$

$$\lambda f'''_{1n}(\lambda) - \frac{1}{\lambda}[1 - \nu + (2+\nu)n^2] f'_{1n}(\lambda) + \frac{3n^2}{\lambda^2} f_{1n}(\lambda) = 0 \tag{18}$$

where

$$L_n(\,) = \left(\frac{d^2}{dx^2} + \frac{1}{x}\frac{d}{dx} - \frac{n^2}{x^2}\right)(\,); \qquad L_n^2 = L_n L_n(\,).$$

The description of the buckling problem was completed by requiring that

$$\lim_{x \to 0} w_{1n}, f_{1n}, xw'_{1n}, xf'_{1n} = 0. \tag{19}$$

These conditions make the apex deflection single valued, and limit the severity of the expected singularity in the membrane forces and bending moments.

The smallest value of p for which equations (13)–(19) admit a solution, for any integer n, is the critical load for bifurcation buckling. Bifurcation will, of course, be the controlling phenomenon only if it occurs before axisymmetric snap-buckling.

Numerical results

The critical load for asymmetric buckling was calculated numerically over a large range of the geometry parameter λ. A value of $\frac{1}{3}$ was used for Poisson's ratio. In the numerical

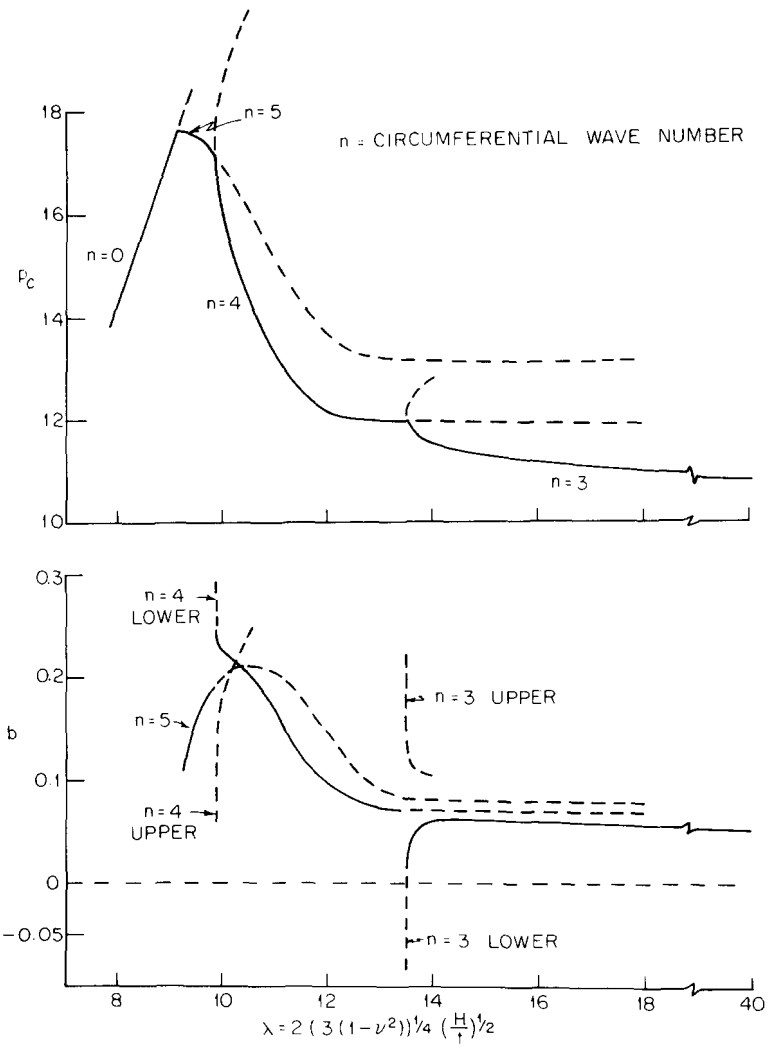

FIG. 4. Buckling and post-buckling of clamped spherical cap under concentrated load.

procedure the shell meridian was divided into equal sub-intervals, and central difference formulas were used to approximate the derivatives in equation (13)–(19). The critical load is the smallest value of p for which the determinant of coefficients of the resulting linear algebraic system vanishes. The axisymmetric equations (7)–(11) must, of course, be solved in order to evaluate this determinant. The method used to solve the axisymmetric problem, and the details of the procedure used to locate the critical load are given in Appendix B. The results are displayed in the top half of Fig. 4. For $\lambda < 7{\cdot}8$ no evidence of bifurcation or axisymmetric snap-buckling was found. For $7{\cdot}8 < \lambda < 9{\cdot}2$ a local maximum on the axisymmetric load–deflection curve was encountered with no prior evidence of bifurcation. These buckling loads were previously obtained by Mescall [5, 6]. The maxima are quite gentle and approach a point of inflection as λ tends to 7·8. For $\lambda > 9{\cdot}2$ asymmetric bifurcation occurs before axisymmetric snap-buckling. The solid curve represents the critical load. The dashed curves, which represent higher eigenvalues of the buckling equations, have been included for completeness. The mode shape associated with the critical load has three, four, or five circumferential waves depending on the value of λ. As λ tends to large values the critical load approaches a limiting value of 10·8. For such λ the disturbance introduced by the load is confined to the region near the apex, hence this limiting value can be taken as the buckling load for a very thin complete sphere under diametrically opposed point loads. In Fig. 5 an example of the radial mode shape associated with the critical load is shown. The single intermediate node was a characteristic property. A comparison of the above results with available experimental data is presented below in the Discussion.

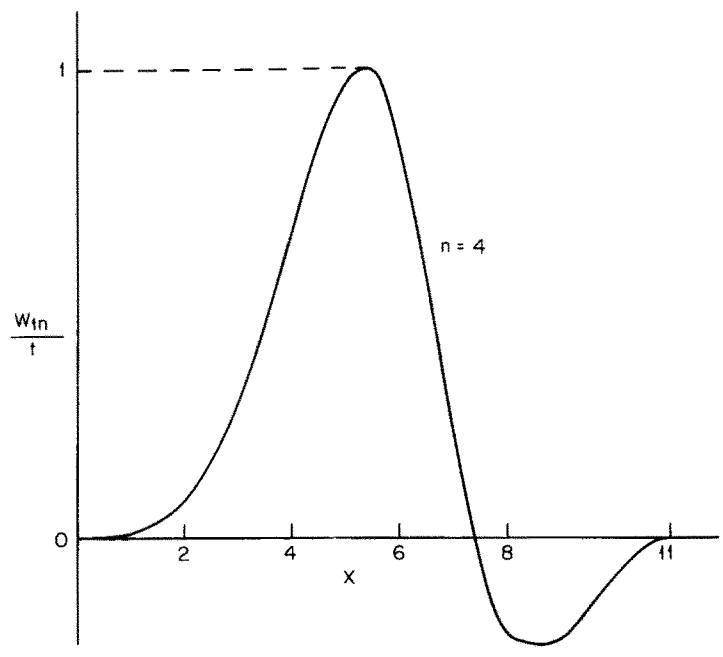

FIG. 5. Buckling mode shape $\lambda = 11$.

INITIAL POST-BUCKLING BEHAVIOR

A general method for analyzing initial post-buckling behavior is described in Appendix A. It is an extension of work by Budiansky and Hutchinson [13], and Budiansky [14]. The work of these authors is, in turn, based on an original analysis by Koiter [15, 16]. The application of this method will yield the initial slope of the bifurcation path, and will also show whether buckling of the point-loaded spherical cap is sensitive to small initial geometric imperfections.

Application of the general theory

Following the procedure developed in Appendix A it will be assumed that the vertical deflection and stress function in a slightly buckled state can be written in the form

$$\begin{Bmatrix} w \\ f \end{Bmatrix} = \begin{Bmatrix} \int_x^\lambda \Theta \, dx \\ \int_0^x \Phi \, dx \end{Bmatrix} + \xi \begin{Bmatrix} w_1 \\ f_1 \end{Bmatrix} + \xi^2 \begin{Bmatrix} w_2 \\ f_2 \end{Bmatrix} + \dots \tag{20}$$

where (Θ, Φ) is the axisymmetric solution at the given load, (w_1, f_1) is the buckling load normalized with respect to the thickness, and ξ is a scalar parameter. It is shown in Appendix A that there is no loss of generality in assuming that (w_2, f_2) and the coefficients of higher powers of ξ are orthogonal to (w_1, f_1) in some sense. The choice of this orthogonality condition will lead to a precise definition of ξ. It is a consequence of the general theory that if (20) is asymptotically valid for $\xi \ll 1$, the deviation from the critical load can be expressed in the form

$$\frac{p}{p_c} = 1 + a\xi + b\xi^2 + \dots \tag{21}$$

also asymptotically valid for small ξ. It is evident that $a = 0$ for the spherical cap because a change in the sign of ξ is equivalent to rotating the cap through π/n degrees, and this cannot change the sign of the deviation from the critical load. It is the sign of b which will determine whether the load initially increases or decreases after buckling. Note that (21) implies

$$\begin{Bmatrix} \Theta \\ \Phi \end{Bmatrix} = \begin{Bmatrix} \Theta \\ \Phi \end{Bmatrix}_c + O(\xi^2)$$

where the subscript c means evaluation at the critical load.

A formula for b is derived in Appendix A. In addition to the axisymmetric solution and the buckling mode it involves the functions w_2 and f_2. An appropriate boundary value problem for these functions can be derived by substituting (20) in equations (1)–(6). After using the definitions of (Θ, Φ) and (w_1, f_1) the resulting equations can be divided through by ξ^2, and ξ allowed to approach zero to obtain

$$\nabla^4 w_2 - \nabla^2 f_2 + \left(\frac{1}{x} f_2' + \frac{1}{x^2} \dot{f}_2\right)\Theta_c' - \frac{1}{x} w_2'' \Phi_c + \frac{1}{x} f_2'' \Theta_c - \left(\frac{1}{x} w_2' + \frac{1}{x^2} \dot{w}_2\right)\Phi_c'$$
$$= \left(\frac{1}{x} f_1' + \frac{1}{x^2} \dot{f}_1\right) w_1'' + \left(\frac{1}{x} w_1' + \frac{1}{x^2} \dot{w}_1\right) f_1'' - 2\left(\frac{1}{x} \dot{f}_1' - \frac{1}{x^2} \dot{f}_1\right)\left(\frac{1}{x} \dot{w}_1' - \frac{1}{x^2} \dot{w}_1\right) \tag{22}$$

$$\nabla^4 f_2 + \nabla^2 w_2 - \left(\frac{1}{x}w_2' + \frac{1}{x^2}\dot{w}_2\right)\Theta_c' - \frac{1}{x}w_2''\Theta_c = \left(\frac{1}{x}\dot{w}_1' - \frac{1}{x^2}\dot{w}_1\right)^2 - \left(\frac{1}{x}w_1' + \frac{1}{x^2}\ddot{w}_1\right)w_1'' \quad (23)$$

plus boundary conditions (3)–(6) on (w_2, f_2). By substituting the known form of (w_1, f_1) in the right hand sides of (22) and (23) it is easily seen that (w_2, f_2) must be of the form

$$\begin{Bmatrix} w_2 \\ f_2 \end{Bmatrix} = \begin{Bmatrix} -\int^x \beta \, dx \\ \int^x \psi \, dx \end{Bmatrix} + \begin{Bmatrix} \rho(x) \\ \chi(x) \end{Bmatrix} \cos 2n\theta + C \begin{Bmatrix} w_{1n} \\ f_{1n} \end{Bmatrix} \cos n\theta \quad (24)$$

where C is an arbitrary constant which can be set to zero with no loss of generality. It is easily shown that (β, ψ) and (ρ, χ) satisfy respectively

$$(x\beta')' - \left(\frac{1}{x} + \Phi_c\right)\beta + (x - \Theta_c)\psi = g_1(x) \quad (25)$$

$$(x\psi')' - \frac{1}{x}\psi - (x - \Theta_c)\beta = g_2(x) \quad (26)$$

$$\beta(\lambda) = 0 \quad (27)$$

$$\lambda\psi'(\lambda) - \nu\psi(\lambda) = 0 \quad (28)$$

where

$$g_1(x) = \frac{1}{2}\left[n^2\left(\frac{w_{1n}f_{1n}}{x}\right)' - w_{1n}'f_{1n}'\right]$$

$$g_2(x) = \frac{1}{4}\left[n^2\left(\frac{w_{1n}^2}{x}\right)' - (w_{1n}')^2\right]$$

and

$$L_{2n}^2(\rho) - L_{2n}(\chi) + \left(\frac{1}{x}\chi' - \frac{4n^2}{x^2}\chi\right)\Theta_c' - \frac{1}{x}\rho''\Phi_c + \frac{1}{x}\chi''\Theta_c - \left(\frac{1}{x}\rho' - \frac{4n^2}{x^2}\rho\right)\Phi_c' = h_1(x) \quad (29)$$

$$L_{2n}^2(\chi) + L_{2n}(\rho) - \left(\frac{1}{x}\rho' - \frac{4n^2}{x^2}\rho\right)\Theta_c' - \frac{1}{x}\rho''\Theta_c = h_2(x) \quad (30)$$

$$\rho(\lambda) = 0 \quad (31)$$

$$\rho'(\lambda) = 0 \quad (32)$$

$$\chi''(\lambda) - \frac{\nu}{\lambda}\chi'(\lambda) + \frac{4n^2\nu}{\lambda^2}\chi(\lambda) = 0 \quad (33)$$

$$\lambda\chi'''(\lambda) - \frac{1}{\lambda}[1 - \nu + 4(2 + \nu)n^2]\chi'(\lambda) + \frac{12n^2}{\lambda^2}\chi(\lambda) = 0 \quad (34)$$

where

$$h_1(x) = \frac{1}{2}\left[\left(\frac{1}{x}f'_{1n}-\frac{n^2}{x^2}f_{1n}\right)w''_{1n}+\left(\frac{1}{x}w'_{1n}-\frac{n^2}{x^2}w_{1n}\right)f''_{1n}\right.$$
$$\left.+2n^2\left(\frac{1}{x}f'_{1n}-\frac{1}{x^2}f_{1n}\right)\left(\frac{1}{x}w'_{1n}-\frac{1}{x^2}w_{1n}\right)\right]$$
$$h_2(x) = -\frac{1}{2}\left[n^2\left(\frac{1}{x}w'_{1n}-\frac{1}{x^2}w_{1n}\right)^2+\left(\frac{1}{x}w'_{1n}-\frac{n^2}{x^2}w_{1n}\right)w''_{1n}\right].$$

To complete the description of the boundary value problems for (β, ψ) and (ρ, χ) it was required that

$$\lim_{x\to 0}\beta, \psi, \rho, \chi, x\rho'', x\chi'' = 0.$$

The formula for b derived in Appendix A involves integrals over the shell base plane. After carrying out the θ integration it can be shown by integration by parts that this formula reduces to

$$b = \frac{1}{p_c w_2(0)}\int_0^\lambda [\beta g_1 - \psi g_2 - \tfrac{1}{2}x(\rho h_1 - \chi h_2)]\,dx. \tag{35}$$

In deriving (35) use has been made of the fact that

$$\int_0^\lambda \left[\left(\frac{\partial\Theta}{\partial p}\right)_c g_1 - \left(\frac{\partial\Phi}{\partial p}\right)_c g_2\right] dx = -\int_0^\lambda \beta\,dx = -w_2(0).$$

This relation can be verified by substituting for g_1 and g_2 from (25) and (26), and by making use of the equations obtained from (7)–(11) by differentiation with respect to p. The fractional change in the slope of the load–apex deflection path which accompanies bifurcation can be expressed in terms of b and w_2. Let $\bar{\Delta}$ and Δ denote respectively the slope of the axisymmetric equilibrium path, and the slope of the bifurcation path at p_c. Then, directly from (20) and (21), it can be shown that

$$\frac{\Delta}{\bar{\Delta}} = \frac{1}{1+\gamma}$$

where

$$\gamma = \frac{w_2(0)}{bp_c}\bar{\Delta}.$$

Numerical results

The numerical solution of equations (25)–(34) was accomplished by finite differencing and the use of Potter's method [17], which is described in Appendix B. The integrals required for the final evaluation of b and $w_2(0)$ were computed by Simpson's rule. The results for b and $\Delta/\bar{\Delta}$ are shown in the bottom half of Fig. 4 and Fig. 6 respectively. The plotted values of b are to be used in conjunction with the equation

$$\frac{p}{p_c} = 1 + b\left(\frac{\delta}{t}\right)^2$$

where $\delta(=\xi t)$ is the amplitude of the buckling mode contribution to the vertical deflection. The solid curves represent the values calculated at the critical load, while the dashed portions correspond to the higher eigenvalues shown in the top half of Fig. 4. On this eigenvalue plot it is seen that the $n = 4$ and $n = 3$ curves have vertical tangents at $\lambda = 9{\cdot}9$ and $13{\cdot}5$ respectively. The curves marked "lower" and "upper" in the b plot correspond to the branches of the eigenvalue curves lying below and above a horizontal line through the point of vertical tangency. It is shown in Appendix A that the formula for b would be expected to become singular at such points. From a practical standpoint the most important observation to be made from the b plot is that the value corresponding to the critical load is positive. This means that the load will initially increase after buckling. As shown in Appendix A it also means that the spherical cap under point load is imperfection-insensitive in the sense that a small initial geometric imperfection would not be expected to trigger snap-buckling at a load less than the classical critical load.

In Fig. 6 only the value of $\Delta/\bar{\Delta}$ corresponding to the critical load has been plotted. The curve reveals the fact that the maximum initial reduction of the slope of the load-apex deflection curve is about 30%. This is the value approached as λ tends to large values, and

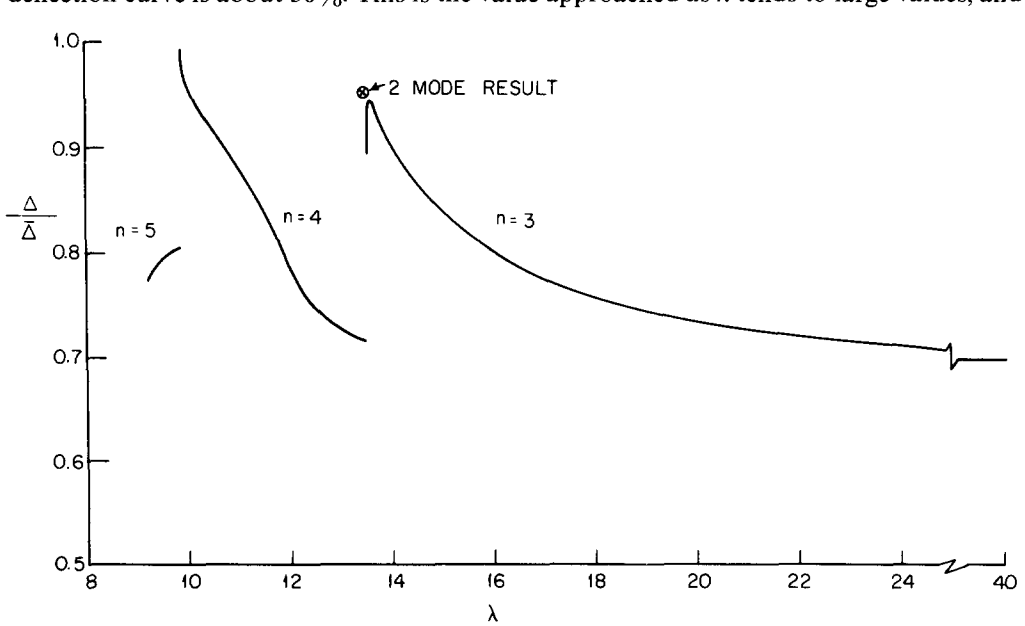

FIG. 6. Reduction in slope of load–apex deflection curve at p_c.

thus can be applied to the limiting case of a very thin complete sphere. A discontinuity is associated with the transition between regions in which the buckling mode has a different number of circumferential waves. At the transition points the analysis must be modified to account for the fact that the buckling mode is not unique. It was found that the modified equations admit solutions which say that the cap buckles purely in one mode or the other. The possibility of buckling in a shape corresponding to a non-trivial linear combination of the two modes was investigated numerically. No such solution was found at the 5–4 transition point. At the 4–3 transition, however, it was found that the cap could buckle in a shape to which the $n = 4$ and $n = 3$ modes contribute in roughly a one to four ratio. The corresponding value of $\Delta/\bar{\Delta}$ is shown on Fig. 6. It is possible that the proximity of the transition

points to the previously mentioned singular points had an adverse effect on the numerical accuracy of the two-mode calculation.

DISCUSSION

The results of the analysis presented in the preceding sections may be summarized as follows. For λ greater than 9·2 the deflection of a clamped spherical cap under concentrated load will become asymmetric at a load below the critical load for axisymmetric snap-buckling. Depending on the value of λ the initial appearance of asymmetry will be characterized by a deflection pattern having three, four, or five circumferential waves. On a plot of load vs. apex deflection the bifurcation equilibrium path has a positive initial slope which is at most about 30% less than the slope of the axisymmetric path at the critical load. A spherical cap with a small initial geometric imperfection would be expected to behave in qualitatively the same manner as the perfect cap. In particular the presence of the imperfection would not be expected to cause snap-buckling at a load below the critical load for the perfect structure.

The experimental data reported in [7], [8] and [18] give qualitative support to the above results. Penning and Thurston [8] and Penning [18] tested specimens having nominal λ values of 5, 8, 12, 16, and 20. At $\lambda = 5$ and 8 there was no evidence of snap-buckling or asymmetric behavior. For $\lambda = 12$, 16, and 20 bifurcation into an asymmetric deflection pattern did occur. In fact a steady progression of three, four, and five lobed patterns was observed as the load was increased. For $\lambda = 16$ and 20 these results correlate with the behavior implied by the eigenvalue plot in Fig. 4, where it is seen that for λ greater than 13·5 eigenvalues corresponding to three, four, and five circumferential waves appear in succession. There is some discrepancy at $\lambda = 12$ where the present theory predicts that the initial appearance of asymmetry would be characterized by four circumferential waves. Asymmetric behavior of the clamped cap is also reported in [7]. The authors state that with increasing load the axisymmetric dimple increased in size and gradually changed into a square or hexagon with rounded corners.

The experiments referred to above do not include a measurement of the load at which asymmetric deflection first appeared, but they do indicate that the initial appearance of asymmetry is associated with a rising load–apex deflection curve. The fact that the asymmetry does develop gradually in a program of increasing load would make the critical load for asymmetric buckling a difficult quantity to obtain experimentally. On several of the experimental load–deflection curves presented in [8] and [18], however, the authors indicate the nature of the deflection at three or four different load values including one at which it was axisymmetric. This made it possible to bracket the load at which asymmetric deflection started to develop. At $\lambda = 16$ and 20 the critical loads predicted by the present theory fall within the bounds deduced in this manner, while at $\lambda = 12$ the predicted value is somewhat higher than the smallest load at which a well established asymmetric deflection is reported.

REFERENCES

[1] C. B. Biezeno, Über die Bestimmung der Durchschlagkraft einer schwachgekrummten kreisformigen Platte. *Z. angew. Math. Mech.* **15**, 10 (1935).

[2] W. Z. Chien and H. C. Hu, On the snapping of a thin spherical cap. *Proc. 9th Int. Congr. appl. Mech.* **6**, 309 (1957).

[3] D. G. ASHWELL, On the large deflection of a spherical shell with an inward point load. *Proc. Symp. Theory Thin Elastic Shells*. North Holland (1959).
[4] R. R. ARCHER, On the numerical solution of the nonlinear equations for shells of revolution. *J. Math. Phys.* **40**, 165 (1962).
[5] J. F. MESCALL, Large deflection of spherical shells under concentrated loads. *J. appl. Mech.* **32**, 936 (1965).
[6] J. F. MESCALL, On the numerical analysis of the nonlinear axisymmetric equations for shells of revolution. Tech. Rpt. 64-20, U.S. Army Materials Research Agency (1964).
[7] R. M. EVAN-IWANOWSKI, H. S. CHENG and T. C. LOO, Experimental investigations on deformations and stability of spherical shells subjected to concentrated loads at the apex. *Proc. 4th U.S. Natn. Congr. appl. Mech.* p. 563 (1962).
[8] F. A. PENNING and G. A. THURSTON, The stability of shallow spherical shells under concentrated load. NASA Contract Rpt. 265 (1965).
[9] K. MARGUERRE, Zur Theorie der gekrümmten Platte grosser Formanderung. *Proc. 5th Int. Congr. appl. Mech.* p. 93 (1938).
[10] B. BUDIANSKY and J. W. HUTCHINSON, A survey of some buckling problems. *AIAA Jnl* **4**, 1505 (1966).
[11] D. BUSHNELL, Bifurcation phenomena in spherical shells under concentrated loads, paper presented at the *AIAA/ASME 8th Struct., Structural Dynamics Mater. Conf.* Palm Springs, California, March 29–31 (1967).
[12] N. C. HUANG, Unsymmetrical buckling of thin shallow spherical shells. *J. appl. Mech.* **31**, 447 (1964).
[13] B. BUDIANSKY and J. W. HUTCHINSON, Dynamic buckling of imperfection sensitive structures, *Proc. 11th Int. Congr. appl. Mech.* p. 636 (1964).
[14] B. BUDIANSKY, Dynamic buckling of elastic structures: criteria and estimates. *Proc. Int. Conf. Dynamic Stability Structures*. Pergamon Press (1965).
[15] W. T. KOITER, On the stability of elastic equilibrium (in Dutch). Thesis, Delft. H. J. Paris (1945).
[16] W. T. KOITER, Elastic stability and post-buckling behavior, *Proc. Symp. Nonlinear Problems*, edited by R. E. LANGER, p. 257. Univ. of Wisc. Press (1963).
[17] M. L. POTTERS, A matrix method for the solution of a second order difference equation in two variables. Rept. MR 19, Mathematich Centrum, Amsterdam, Holland (1955).
[18] F. A. PENNING, Nonaxisymmetric behavior of shallow shells loaded at the apex. *J. appl. Mech.* **33**, 699 (1966).
[19] J. M. T. THOMPSON, Discrete branching points in the general theory of elastic stability. *J. Mech. Phys. Solids* **13**, 295 (1965).
[20] G. A. THURSTON, Newton's method applied to problems in nonlinear mechanics. *J. appl. Mech.* **32**, 383 (1965).
[21] R. E. BLUM and R. E. FULTON, A modification of Potters' method for solving eigenvalue problems involving tridiagonal matrices. *AIAA Jnl* **4**, 2231 (1966).

APPENDIX A

GENERAL THEORY OF INITIAL POST-BUCKLING BEHAVIOR

For some years now a theory of initial post-buckling behavior, developed by Koiter [15, 16], has been available. It is essentially a perturbation technique which relies on the principle of stationary potential energy. In recent work Budiansky and Hutchinson [13] and Budiansky [14] have derived equivalent results by writing the field equations directly in variational form with the aid of the principle of virtual work. This approach develops the theory in a form which is especially convenient for application. Their work is limited, however, by the restriction that the pre-buckling behavior of the structure be linearly proportional to the load. This is the case in many instances—the cylinder under axial compression, the sphere under uniform pressure—but it is not the case for the clamped spherical cap. In this Appendix the Budiansky–Hutchinson approach will be generalized to account for non-linear pre-buckling behavior. One additional reference which deserves mention is a recent paper by Thompson [19] in which an approach similar to Koiter's is used to analyze the post-buckling behavior of structures whose equilibrium states can be described by discrete coordinates.

Buckling and post-buckling theory of the perfect structure

For the sake of simplicity and generality a highly abbreviated notation, introduced in [14], will be used in the analysis to follow. Let $\mathbf{u}, \boldsymbol{\varepsilon}, \mathbf{q}$, and $\boldsymbol{\sigma}$ denote generalized displacement, strain, load, and stress variables. Each of these symbols can be thought of as denoting a vector function, with the number and identity of its components determined by the specific problem under consideration. These variables are assumed to satisfy the strain-displacement law

$$\boldsymbol{\varepsilon} = L_1(\mathbf{u}) + \tfrac{1}{2}L_2(\mathbf{u}) \equiv \mathbf{e} + \tfrac{1}{2}L_2(\mathbf{u}) \tag{A1}$$

and the constitutive law

$$\boldsymbol{\sigma} = H(\boldsymbol{\varepsilon}) \tag{A2}$$

where L_1 and H are linear functionals and L_2 is a quadratic functional. The internal virtual work of stress $\boldsymbol{\sigma}$ through strain variation $\delta\boldsymbol{\varepsilon}$, and the external virtual work of load $\mathbf{q}$ through displacement variation $\delta\mathbf{u}$, integrated over the entire structure, will be denoted by $\boldsymbol{\sigma} \,.\, \delta\boldsymbol{\varepsilon}$ and $\mathbf{q} \,.\, \delta\mathbf{u}$ respectively. It will be assumed that the equilibrium of stress $\boldsymbol{\sigma}$ and load $\mathbf{q}$ (in the presence of displacement $\mathbf{u}$) is guaranteed by the condition

$$\boldsymbol{\sigma} \,.\, \delta\boldsymbol{\varepsilon} = \mathbf{q} \,.\, \delta\mathbf{u} \tag{A3}$$

for all $\delta\mathbf{u}$ which are admissible (i.e. which satisfy the geometric constraints of the problem). Here $\delta\boldsymbol{\varepsilon}$ is the first order strain variation produced by $\delta\mathbf{u}$. If the bilinear functional L_{11} is defined by the relation

$$L_2(\mathbf{u}+\mathbf{v}) = L_2(\mathbf{u}) + 2L_{11}(\mathbf{u}, \mathbf{v}) + L_2(\mathbf{v}) \tag{A4}$$

it follows from (A1) that

$$\delta\boldsymbol{\varepsilon} = L_1(\delta\mathbf{u}) + L_{11}(\mathbf{u}, \delta\mathbf{u}) \equiv \delta\mathbf{e} + L_{11}(\mathbf{u}, \delta\mathbf{u}) \,. \tag{A5}$$

The variational statement of equilibrium (A3) is the converse of the usual principle of virtual work. In addition to the above relations it will be assumed that the structure satisfies the reciprocity law

$$H(\boldsymbol{\varepsilon}_1) \,.\, \boldsymbol{\varepsilon}_2 = H(\boldsymbol{\varepsilon}_2) \,.\, \boldsymbol{\varepsilon}_1 \tag{A6}$$

for all $\boldsymbol{\varepsilon}_1$ and $\boldsymbol{\varepsilon}_2$. The investigation will be limited to loadings which can be represented by $p\mathbf{q}_0$, where $\mathbf{q}_0$ is the loading in some fixed reference state, and p is a scalar parameter.

Let the displacement field associated with a non-buckled equilibrium state of the structure be denoted by $\bar{\mathbf{u}}(p)$. From (A3) $\bar{\mathbf{u}}(p)$ must satisfy

$$\bar{\boldsymbol{\sigma}} \,.\, \delta\bar{\boldsymbol{\varepsilon}} = p\mathbf{q}_0 \,.\, \delta\mathbf{u} \tag{A7}$$

for all admissable $\delta\mathbf{u}$ where

$$\bar{\boldsymbol{\sigma}} = H(\bar{\boldsymbol{\varepsilon}}) = H[\bar{\mathbf{e}} + \tfrac{1}{2}L_2(\bar{\mathbf{u}})]$$

and

$$\delta\bar{\boldsymbol{\varepsilon}} = \delta\mathbf{e} + L_{11}(\bar{\mathbf{u}}, \delta\mathbf{u}) \,.$$

To investigate the possibility of bifurcation buckling at load p_c a solution to (A3) at load $p_c+\Delta p$ is sought in the form

$$\mathbf{u} = \bar{\mathbf{u}}(p_c+\Delta p)+\xi\mathbf{u}_1 \tag{A8}$$

where ξ is a scalar parameter which tends to zero with Δp. Substitution of (A8) into (A3), use of (A7), and consideration of the limit as Δp approaches zero leads to the variational equation

$$\bar{\boldsymbol{\sigma}}_c \cdot L_{11}(\mathbf{u}_1, \delta\mathbf{u})+\boldsymbol{\sigma}_1 \cdot \delta\bar{\boldsymbol{\varepsilon}}_c = 0 \tag{A9}$$

in which

$$\begin{aligned}
\boldsymbol{\sigma}_1 &= H[\mathbf{e}_1+L_{11}(\bar{\mathbf{u}}_c, \mathbf{u}_1)] \\
\delta\bar{\boldsymbol{\varepsilon}}_c &= \delta\mathbf{e}+L_{11}(\bar{\mathbf{u}}_c, \delta\mathbf{u}) \\
\bar{\mathbf{u}}_c &= \bar{\mathbf{u}}(p_c); \qquad \bar{\boldsymbol{\sigma}}_c = \bar{\boldsymbol{\sigma}}(p_c).
\end{aligned}$$

Equation (A9) is the variational statement of the eigenvalue problem for bifurcation buckling. In the analysis to follow p_c will denote the lowest eigenvalue of (A9), and it will be assumed that it corresponds to a unique buckling mode $\mathbf{u}_1$.

In a slightly buckled state the displacement can always be written in the form

$$\mathbf{u}(p) = \bar{\mathbf{u}}(p)+\xi\mathbf{u}_1+\mathbf{w} \tag{A10}$$

where $\mathbf{u}_1$ has been normalized in some manner, and ξ is again a scalar parameter. The parameter ξ can now be defined precisely by requiring, with no loss of generality, that $\mathbf{w}$ be orthogonal to $\mathbf{u}_1$ in some sense. In particular, if Q_{11} is a bilinear operator satisfying the condition $Q_{11}(\mathbf{u}_1, \mathbf{u}_1) \neq 0$, the orthogonality condition

$$Q_{11}(\mathbf{u}_1, \mathbf{w}) = 0 \tag{A11}$$

implies

$$\xi = \frac{Q_{11}(\mathbf{u}-\bar{\mathbf{u}}, \mathbf{u}_1)}{Q_{11}(\mathbf{u}_1, \mathbf{u}_1)}.$$

Roughly speaking then, ξ can be regarded as a measure of the "participation" of $\mathbf{u}_1$ in the displacement which has occurred after the initiation of buckling. It is now reasonable to assume that $\mathbf{w}$ can be represented by a perturbation series of the form*

$$\mathbf{w} = \xi^2\mathbf{u}_2+\xi^3\mathbf{u}_3+\ldots.$$

It will be assumed that this series is at least asymptotically valid for $\xi \ll 1$. The displacement (A10) now takes the form

$$\mathbf{u}(p) = \bar{\mathbf{u}}(p)+\xi\mathbf{u}_1+\xi^2\mathbf{u}_2+\xi^3\mathbf{u}_3+\ldots. \tag{A12}$$

* It is easily shown that a first order term in ξ would violate the orthogonality condition (A11) because its coefficient would have to satisfy the buckling equation (A9), and hence be a multiple of $\mathbf{u}_1$.

Corresponding expressions for strain and stress can be found by substituting (A12) in (A1) and (A2). Thus

$$\begin{aligned}\boldsymbol{\varepsilon}(p) = \bar{\boldsymbol{\varepsilon}}(p) &+ \xi[\mathbf{e}_1 + L_{11}(\bar{\mathbf{u}}, \mathbf{u}_1)] \\ &+ \xi^2[\mathbf{e}_2 + \tfrac{1}{2}L_2(\mathbf{u}_1) + L_{11}(\bar{\mathbf{u}}, \mathbf{u}_2)] \\ &+ \xi^3[\mathbf{e}_3 + L_{11}(\mathbf{u}_1, \mathbf{u}_2) + L_{11}(\bar{\mathbf{u}}, \mathbf{u}_3)] + \dots \end{aligned} \tag{A13}$$

where $\mathbf{e}_n = L_1(\mathbf{u}_n)$. It will now be assumed that $\bar{\mathbf{u}}(p)$ can be expanded in the Taylor series

$$\bar{\mathbf{u}}(p) = \bar{\mathbf{u}}_c + (p - p_c)\bar{\mathbf{u}}_c' + \frac{(p-p_c)^2}{2}\bar{\mathbf{u}}_c'' + \dots \tag{A14}$$

where primes denote differentiation with respect to p. In addition it will be assumed that p/p_c admits the asymptotic representation

$$p/p_c = 1 + a\xi + b\xi^2 + \dots . \tag{A15}$$

With these assumptions $\boldsymbol{\varepsilon}$ and $\boldsymbol{\sigma}$ can be written in the expanded form

$$\begin{Bmatrix} \boldsymbol{\varepsilon}(p) \\ \boldsymbol{\sigma}(p) \end{Bmatrix} = \begin{Bmatrix} \bar{\boldsymbol{\varepsilon}}(p) \\ \bar{\boldsymbol{\sigma}}(p) \end{Bmatrix} + \xi \begin{Bmatrix} \boldsymbol{\varepsilon}_1 \\ \boldsymbol{\sigma}_1 \end{Bmatrix} + \xi^2 \begin{Bmatrix} \boldsymbol{\varepsilon}_2 \\ \boldsymbol{\sigma}_2 \end{Bmatrix} + \xi^3 \begin{Bmatrix} \boldsymbol{\varepsilon}_3 \\ \boldsymbol{\sigma}_3 \end{Bmatrix} + \dots \tag{A16}$$

where

$$\begin{aligned} \boldsymbol{\varepsilon}_1 &= \mathbf{e}_1 + L_{11}(\bar{\mathbf{u}}_c, \mathbf{u}_1) \\ \boldsymbol{\varepsilon}_2 &= \mathbf{e}_2 + L_{11}(\bar{\mathbf{u}}_c, \mathbf{u}_2) + \tfrac{1}{2}L_2(\mathbf{u}_1) + (ap_c)L_{11}(\bar{\mathbf{u}}_c', \mathbf{u}_1) \\ \boldsymbol{\varepsilon}_3 &= \mathbf{e}_3 + L_{11}(\bar{\mathbf{u}}_c, \mathbf{u}_3) + L_{11}(\mathbf{u}_1, \mathbf{u}_2) + (bp_c)L_{11}(\bar{\mathbf{u}}_c', \mathbf{u}_1) \\ &\quad + \frac{(ap_c)^2}{2}L_{11}(\bar{\mathbf{u}}_c'', \mathbf{u}_1) + (ap_c)L_{11}(\bar{\mathbf{u}}_c', \mathbf{u}_2) \end{aligned}$$

and $\boldsymbol{\sigma}_n = H(\boldsymbol{\varepsilon}_n)$.

If the displacement field (A12) is perturbed in the shape $\delta\mathbf{u}$ the accompanying strain variation is

$$\delta\boldsymbol{\varepsilon} = \delta\bar{\boldsymbol{\varepsilon}} + \xi L_{11}(\mathbf{u}_1, \delta\mathbf{u}) + \xi^2 L_{11}(\mathbf{u}_2, \delta\mathbf{u}) + \dots . \tag{A17}$$

The equation of equilibrium in a slightly buckled state is obtained by substituting (A16) and (A17) in equation (A3). Then, after simplification with the use of (A7), one obtains

$$\begin{aligned} &\xi[\bar{\boldsymbol{\sigma}} \cdot L_{11}(\mathbf{u}_1, \delta\mathbf{u}) + \boldsymbol{\sigma}_1 \cdot \delta\bar{\boldsymbol{\varepsilon}}] + \xi^2[\bar{\boldsymbol{\sigma}} \cdot L_{11}(\mathbf{u}_2, \delta\mathbf{u}) + \boldsymbol{\sigma}_1 \cdot L_{11}(\mathbf{u}_1, \delta\mathbf{u}) + \boldsymbol{\sigma}_2 \cdot \delta\bar{\boldsymbol{\varepsilon}}] \\ &\quad + \xi^3[\bar{\boldsymbol{\sigma}} \cdot L_{11}(\mathbf{u}_3, \delta\mathbf{u}) + \boldsymbol{\sigma}_1 \cdot L_{11}(\mathbf{u}_2, \delta\mathbf{u}) + \boldsymbol{\sigma}_2 \cdot L_{11}(\mathbf{u}_1, \delta\mathbf{u}) \\ &\quad + \boldsymbol{\sigma}_3 \cdot \delta\bar{\boldsymbol{\varepsilon}}] + \dots = 0 . \end{aligned} \tag{A18}$$

From (A18) explicit formulas for the coefficients a and b in (A15) can be found. This is accomplished by expanding the barred quantities in (A18) in powers of ξ with the help of (A14, 15). Then $\delta\mathbf{u}$ is set equal to $\mathbf{u}_1$, and the result simplified with the use of

$$\bar{\boldsymbol{\sigma}}_c \cdot L_{11}(\mathbf{u}_1, \mathbf{u}_n) + \boldsymbol{\sigma}_1 \cdot [\mathbf{e}_n + L_{11}(\bar{\mathbf{u}}_c, \mathbf{u}_n)] = 0, \qquad n = 1, 2, \dots \tag{A19}$$

which is a direct consequence of equation (A9). Equating to zero the coefficient of the lowest order (quadratic) term in ξ then gives

$$ap_c B_2(\mathbf{u}_1) + \tfrac{3}{2}\boldsymbol{\sigma}_1 \cdot L_2(\mathbf{u}_1) = 0$$

where

$$B_2(\mathbf{u}_1) = \bar{\boldsymbol{\sigma}}_c' \cdot L_2(\mathbf{u}_1) + 2\boldsymbol{\sigma}_1 \cdot L_{11}(\bar{\mathbf{u}}_c', \mathbf{u}_1) . \tag{A20}$$

Thus, assuming $B_2(\mathbf{u}_1) \neq 0$,

$$a = -\frac{\tfrac{3}{2}\boldsymbol{\sigma}_1 \cdot L_2(\mathbf{u}_1)}{p_c B_2(\mathbf{u}_1)} \tag{A21}$$

The formula for b is obtained by equating to zero the coefficient of the ξ^3 term. For simplicity and because it represents the most important instance, the formula will be written only for the case in which $a = 0$. Then

$$b = -\frac{\boldsymbol{\sigma}_2 \cdot L_2(\mathbf{u}_1) + 2\boldsymbol{\sigma}_1 \cdot L_{11}(\mathbf{u}_1, \mathbf{u}_2)}{p_c B_2(\mathbf{u}_1)} . \tag{A22}$$

To calculate b the function $\mathbf{u}_2$ must be found. An equation for this purpose can be obtained directly from (A18) by again making use of (A14, 15). The result (for $a = 0$) is

$$\bar{\boldsymbol{\sigma}}_c \cdot L_{11}(\mathbf{u}_2, \delta\mathbf{u}) + \boldsymbol{\sigma}_2 \cdot \delta\bar{\boldsymbol{\varepsilon}}_c = -\boldsymbol{\sigma}_1 \cdot L_{11}(\mathbf{u}_1, \delta\mathbf{u}) . \tag{A23}$$

This equation leaves $\mathbf{u}_2$ undetermined to the extent of an arbitrary multiple of $\mathbf{u}_1$. By direct substitution in (A22) it is readily seen that when $a = 0$ all such solutions give the same value for b. For the cases $a \neq 0$ or $a = 0, b \neq 0$ formula (A21) or (A22) is sufficient to determine the variation of p/p_c with ξ immediately after buckling. Note that in the latter case the sign of b alone determines whether the load initially increases or decreases.

In applying formula (A22) to the spherical cap problem it was found that $B_2(\mathbf{u}_1)$ vanished under certain circumstances. Re-examination of the theory led to the following result. Suppose that after non-dimensionalization the field equations contain, in addition to the load parameter p, a parameter λ (typically characterizing the geometry of the structure). Let C denote the curve formed when one of the eigenvalues of (A9) is plotted against λ, and let $\lambda(p)$ be the functional representation of C. Along C the buckling mode $\mathbf{u}_1$ can be regarded as a function of p, and with $\delta\mathbf{u} = \mathbf{u}_1(p)$ (A9) gives

$$\bar{\boldsymbol{\sigma}}(p, \lambda) \cdot L_2[\mathbf{u}_1(p)] + \boldsymbol{\sigma}_1(p, \lambda) \cdot \boldsymbol{\varepsilon}_1(p, \lambda) = 0$$

on C. Let the function on the left-hand side of this equation be denoted by $g(p, \lambda)$, and note that the derivative of g with respect to distance along C must also vanish on C. Now suppose there exists a point (p_0, λ_0) on C at which $\lambda'(p)$ vanishes. At this point the derivative of g along C will equal the partial of g with respect to p at constant λ. Thus

$$\frac{\partial g}{\partial p}(p_0, \lambda_0) = 0 .$$

Now by a second application of (A9) with $\delta\mathbf{u} = \mathbf{u}_1'(p_0)$ it can be shown that

$$B_2[\mathbf{u}_1(p_0)] = \frac{\partial g}{\partial p}(p_0, \lambda_0) . \tag{A24}$$

Thus $B_2(\mathbf{u}_1)$ will vanish at p_0, and formulas (A21) and (A22) for a and b will become singular.

The imperfect structure

Following previous investigators [13–16, 19] it is of interest to see how the above theory relates to the case in which the structure has a small initial stress-free geometric imperfection $\hat{\mathbf{u}}$. The strain can be re-defined in terms of the *additional* displacement $\mathbf{u}$ by

$$\boldsymbol{\varepsilon} = L_1(\mathbf{u}) + \tfrac{1}{2}L_2(\mathbf{u}) + L_{11}(\hat{\mathbf{u}}, \mathbf{u}).$$

It is reasonable to presume that the behavior will be most sensitive to an imperfection in the shape of the buckling mode. Thus $\hat{\mathbf{u}}$ will be taken in the form $\hat{\xi}\mathbf{u}_1$, where $\hat{\xi}$ is a scalar parameter. If only the lowest order terms in $\hat{\xi}$ are retained the additional displacement can still be represented by (A12). The neglected terms in this procedure are $O(\xi\hat{\xi})$. To the same order in $\hat{\xi}$ the equilibrium equation (A3), with $\delta\mathbf{u} = \mathbf{u}_1$, now gives

$$\begin{aligned}
&\xi[\bar{\boldsymbol{\sigma}} \cdot L_2(\mathbf{u}_1) + \mathbf{S}_1 \cdot \mathbf{E}_1] + \xi^2[\bar{\boldsymbol{\sigma}} \cdot L_{11}(\mathbf{u}_1, \mathbf{u}_2) + \mathbf{S}_1 \cdot (\mathbf{E}_2 + L_2(\mathbf{u}_1))] \\
&\quad + \xi^3[\bar{\boldsymbol{\sigma}} \cdot L_{11}(\mathbf{u}_1, \mathbf{u}_3) + \mathbf{S}_1 \cdot (\mathbf{E}_3 + L_{11}(\mathbf{u}_1, \mathbf{u}_2)) + \mathbf{S}_2 \cdot L_2(\mathbf{u}_1)] + \ldots \\
&= -\hat{\xi}[\bar{\boldsymbol{\sigma}} \cdot L_2(\mathbf{u}_1) + \mathbf{S}_1 \cdot L_{11}(\mathbf{u}_1, \bar{\mathbf{u}})] \qquad \text{(A25)}
\end{aligned}$$

where

$$\begin{aligned}
\mathbf{E}_1 &= \mathbf{e}_1 + L_{11}(\bar{\mathbf{u}}, \mathbf{u}_1) \\
\mathbf{E}_2 &= \mathbf{e}_2 + L_{11}(\bar{\mathbf{u}}, \mathbf{u}_2) + \tfrac{1}{2}L_2(\mathbf{u}_1) \\
\mathbf{E}_3 &= \mathbf{e}_3 + L_{11}(\bar{\mathbf{u}}, \mathbf{u}_3) + L_{11}(\mathbf{u}_1, \mathbf{u}_2)
\end{aligned}$$

and $\mathbf{S}_n = H(\mathbf{E}_n)$. Equation (A25) is an implicit description of the relationship between p and ξ in the presence of imperfection $\hat{\xi}$. It may be expected to be asymptotically valid for sufficiently small ξ and $\hat{\xi}$.

It is of primary interest to determine whether the p–ξ relationship described by (A25) has a local maximum at a load p_s less than the critical load for the perfect structure. A necessary condition for a maximum at $\xi = \xi_s$ is

$$\begin{aligned}
&[\bar{\boldsymbol{\sigma}} \cdot L_2(\mathbf{u}_1) + \mathbf{S}_1 \cdot \mathbf{E}_1]_s + 2\xi_s[\bar{\boldsymbol{\sigma}} \cdot L_{11}(\mathbf{u}_1, \mathbf{u}_2) + \mathbf{S}_1 \cdot (\mathbf{E}_2 + L_2(\mathbf{u}_1))]_s \\
&\quad + 3\xi_s^2[\bar{\boldsymbol{\sigma}} \cdot L_{11}(\mathbf{u}_1, \mathbf{u}_3) + \mathbf{S}_1 \cdot (\mathbf{E}_3 + L_{11}(\mathbf{u}_1, \mathbf{u}_2)) + \mathbf{S}_2 \cdot L_2(\mathbf{u}_1)]_s + \ldots \\
&= 0 \qquad \text{(A26)}
\end{aligned}$$

where the subscript s denotes evaluation at p_s. Now p_s and $\hat{\xi}$ can be regarded as functions of ξ_s satisfying

$$\begin{aligned}
p_s(0) &= p_c \\
\hat{\xi}(0) &= 0.
\end{aligned}$$

Thus it is reasonable to assume that for sufficiently small ξ_s

$$\frac{p_s}{p_c} = 1 + \alpha\xi_s^k \qquad \text{(A27)}$$

$$\hat{\xi} = \beta\xi_s^m. \qquad \text{(A28)}$$

The unknown coefficients and exponents can be found by substituting (A27) and (A28) in (A26) and the equation obtained by evaluating (A25) at ξ_s. Then, for a balance of lowest order terms, it is found that $k = 1$, $m = 2$, $\alpha = 2a$, and

$$\beta = \frac{ap_c B_2(\mathbf{u}_1)}{(\mathbf{S}_1 \cdot \mathbf{e}_1)_c}$$

where the subscript c means evaluation at p_c. These results may now be substituted in (A27) and (A28) and ξ_s eliminated to obtain the asymptotic result

$$\left(1 - \frac{p_s}{p_c}\right)^2 = \frac{4a\hat{\xi}}{p_c} \frac{(\mathbf{S}_1 \cdot \mathbf{e}_1)_c}{B_2(\mathbf{u}_1)} . \tag{A29}$$

For one sign or the other of $a\hat{\xi}$ this equation admits a real-valued solution $p_s < p_c$. If $a = 0$ the balance of lowest order terms in (A25) and (A26) gives $k = 2$, $m = 3$, $\alpha = 3b$, and

$$\beta = \frac{2bp_c B_2(\mathbf{u}_1)}{(\mathbf{S}_1 \cdot \mathbf{e}_1)_c} .$$

This in turn leads to the asymptotic equation

$$\left(1 - \frac{p_s}{p_c}\right)^{3/2} = -\frac{3\sqrt{3}}{2} \frac{\sqrt{(-b)}\hat{\xi}}{p_c} \frac{(\mathbf{S}_1 \cdot \mathbf{e}_1)_c}{B_2(\mathbf{u}_1)} . \tag{A30}$$

Only for $b < 0$ does this equation admit a real-valued solution $p_s < p_c$. In the terminology of [13, 14] structures for which $a \neq 0$, or for which $a = 0$ with $b < 0$ are imperfection-sensitive. That is a small imperfection may be expected to trigger snap-buckling at a load below the critical load of the perfect structure. By the same token structures for which $a = 0$ with $b > 0$ are said to be imperfection-insensitive. Equations (A29) and (A30) are analogous to those derived by Thompson [19] for structures whose equilibrium states can be described by discrete coordinates.

Spherical cap formulas

For a spherical cap the strain–displacement equations are (with $(\,)' \equiv (\partial/\partial r)(\,)$)

$$\varepsilon_r = U' + \frac{r}{R} W' + \tfrac{1}{2}(W')^2 \tag{A31}$$

$$\varepsilon_\theta = \frac{1}{r} U + \frac{1}{r} \dot{V} + \frac{1}{2}\left(\frac{1}{r} \dot{W}\right)^2 \tag{A32}$$

$$\varepsilon_{r\theta} = \frac{1}{2}\left(\frac{1}{r} \dot{U} - \frac{1}{r} V + V' + \frac{1}{R} \dot{W} + \frac{1}{r} \dot{W} W'\right) \tag{A33}$$

$$\kappa_r = -W'' \tag{A34}$$

$$\kappa_\theta = -\frac{1}{r^2} \ddot{W} - \frac{1}{r} W' \tag{A35}$$

$$\kappa_{r\theta} = -\left(\frac{1}{r} \dot{W}\right)' \tag{A36}$$

where ε_r, ε_θ, $\varepsilon_{r\theta}$ are the radial, tangential, and shear strains, κ_r and κ_θ are the curvature changes in the meridional and circumferential planes, $\kappa_{r\theta}$ is the shell twist, and U, V, and W are the horizontal radial, horizontal tangential, and vertical displacements. The principle of virtual work states that if the membrane forces N_r, N_θ, $N_{r\theta}$, and the bending and twisting moments M_r, M_θ, $M_{r\theta}$ (Fig. 3) are in equilibrium with load P, and if the corresponding displacement field is varied in the shape $(\delta U, \delta V, \delta W)$—arbitrary but for the requirement $\delta U = \delta V = \delta W = \delta W' = 0$ at $r = r_0$—then

$$\int_0^{2\pi} \mathrm{d}\theta \int_0^{r_0} r\,\mathrm{d}r[N_r\delta\varepsilon_r + N_\theta\delta\varepsilon_\theta + 2N_{r\theta}\delta\varepsilon_{r\theta} + M_r\delta\kappa_r + M_\theta\delta\kappa_\theta + 2M_{r\theta}\delta\kappa_{r\theta}] = P\delta W(0) \quad \text{(A37)}$$

where $\delta\varepsilon_r$, $\delta\varepsilon_\theta$ etc. are the first order strain variations calculated from (A31)–(A36). In shallow shell theory the membrane forces are derived from a stress function F by

$$N_r = \frac{1}{r}F' + \frac{1}{r^2}\ddot{F}$$

$$N_\theta = F''$$

$$N_{r\theta} = -\left(\frac{1}{r}\dot{F}\right)'.$$

Thus, for a spherical cap

$$\boldsymbol{\sigma} \cdot L_{11}(\mathbf{u}, \delta\mathbf{u}) = \int_0^{2\pi} \mathrm{d}\theta \int_0^{r_0} r\,\mathrm{d}r\left[\left(\frac{1}{r}F' + \frac{1}{r^2}\ddot{F}\right)W'\delta W' + \frac{1}{r^2}F''\dot{W}\delta\dot{W} - \frac{1}{r}\left(\frac{1}{r}\dot{F}\right)'(W'\delta\dot{W} + \dot{W}\delta W')\right]. \quad \text{(A38)}$$

Using (A38) it is a simple matter to express a and b in terms of the functions appearing in the expansion (20). It is then easily verified that $a = 0$ and that the formula for b in terms of non-dimensional variables is

$$b = -\frac{\displaystyle\int_0^{2\pi} \mathrm{d}\theta \int_0^{\lambda} x\,\mathrm{d}x\left[2\left(\frac{1}{x}f_1' + \frac{1}{x^2}\ddot{f}_1\right)w_1'w_2' - \frac{2}{x}\left(\frac{\dot{f}_1}{x}\right)'(w_1'\dot{w}_2 + \dot{w}_1w_2') + \frac{2}{x^2}f_1''\dot{w}_1\dot{w}_2 + \left(\frac{1}{x}f_2' + \frac{1}{x^2}\ddot{f}_2\right)(w_1')^2 - \frac{2}{x}\left(\frac{\dot{f}_2}{x}\right)'\dot{w}_1w_1' + \frac{1}{x^2}f_2''\dot{w}_1^2\right]}{p_c\displaystyle\int_0^{2\pi} \mathrm{d}\theta \int_0^{\lambda} x\,\mathrm{d}x\left\{\frac{1}{x}\left(\frac{\partial\Phi}{\partial p}\right)_c(w_1')^2 + \frac{1}{x^2}\left(\frac{\partial\Phi'}{\partial p}\right)_c\dot{w}_1^2 - 2\left[\left(\frac{1}{x}f_1' + \frac{1}{x^2}\ddot{f}_1\right)w_1' - \frac{1}{x}\left(\frac{\dot{f}_1}{x}\right)'\dot{w}_1\right]\left(\frac{\partial\Theta}{\partial p}\right)_c\right\}}. \quad \text{(A39)}$$

APPENDIX B
NUMERICAL PROCEDURE

Axisymmetric problem

A technique known as Newton's method was used to solve the non-linear system (7)–(11). This method has been described by Thurston [20], and has previously been applied to

the spherical shell problem by Mescall [6], and by Penning and Thurston [8]. A brief description will be given here for the sake of completeness.

Let $(\tilde{\Theta}, \tilde{\Phi})$ be an estimate of the solution, and denote the difference between it and the exact solution by $(\delta\Theta, \delta\Phi)$. Thus

$$\begin{Bmatrix}\Theta\\ \Phi\end{Bmatrix} = \begin{Bmatrix}\tilde{\Theta}\\ \tilde{\Phi}\end{Bmatrix} + \begin{Bmatrix}\delta\Theta\\ \delta\Phi\end{Bmatrix}. \tag{B1}$$

Now substitute (B1) in equations (7)–(11) and delete quadratic terms in $\delta\Theta$ and $\delta\Phi$ to obtain the system of linear correctional equations

$$(x\delta\Theta')' - \left(\frac{1}{x} + \tilde{\Phi}\right)\delta\Theta + (x - \tilde{\Theta})\delta\Phi = -\left[(x\tilde{\Theta}')' - \frac{1}{x}\tilde{\Theta} + x\tilde{\Phi} - \tilde{\Phi}\tilde{\Theta} + p\right] \tag{B2}$$

$$(x\delta\Phi')' - \frac{1}{x}\delta\Phi - (x - \tilde{\Theta})\delta\Theta = -\left[(x\tilde{\Phi}')' - \frac{1}{x}\tilde{\Phi} - x\tilde{\Theta} + \frac{1}{2}\tilde{\Theta}^2\right] \tag{B3}$$

$$\delta\Theta(\lambda) = 0 \tag{B4}$$

$$\lambda\delta\Phi'(\lambda) - \nu\delta\Phi(\lambda) = 0 \tag{B5}$$

$$\lim_{x\to 0} \delta\Theta, \delta\Phi = 0\,. \tag{B6}$$

In writing equations (B4)–(B6) it has been assumed that $(\tilde{\Theta}, \tilde{\Phi})$ satisfies the homogeneous boundary conditions (9)–(11). Equations (B2)–(B6) are now solved numerically (see below) to obtain an improved estimate of the solution, which can be used to obtain new corrections, and so on until some appropriate convergence criterion is satisfied. The criterion used here was that the correction functions be uniformly less than 0·01 % of the maximum value of the current estimate of the solution. The load–apex deflection curve was efficiently generated by first solving the linearized version of (7)–(11) at a small load ($p = 1$, say) where the linear solution is valid. With this solution as initial estimate the non-linear problem was solved at a slightly higher value of p. The converged result was used as the initial estimate at a somewhat larger p and so on. With an increment of one or two units in p at each step a very satisfactory rate of convergence was obtained.* Figs. 7, 8 and 9 show typical results obtained at $\lambda = 11$. Figure 7 is a plot of load vs. apex deflection, and Figs. 8 and 9 exhibit the vertical deflection, and radial and tangential stress resultants as functions of the meridional coordinate.

The first step in the numerical solution of the linear correctional system (B2)–(B6) was to subdivide the shell meridian with equally spaced mesh points $j = 1, 2, \ldots, N$ and to approximate the derivatives with central difference formulas. Equations (B2) and (B3) can then be written in the matrix form

$$A_j\delta y_{j-1} + B_j\delta y_j + C_j\delta y_{j+1} = d_j, \qquad j = 2, 3, \ldots, N-1 \tag{B7}$$

where

$$y_j = \begin{Bmatrix}\Theta_j\\ \Phi_j\end{Bmatrix},$$

* There was, of course, a dramatic breakdown in convergence associated with the appearance of a local maximum on the load deflection curve.

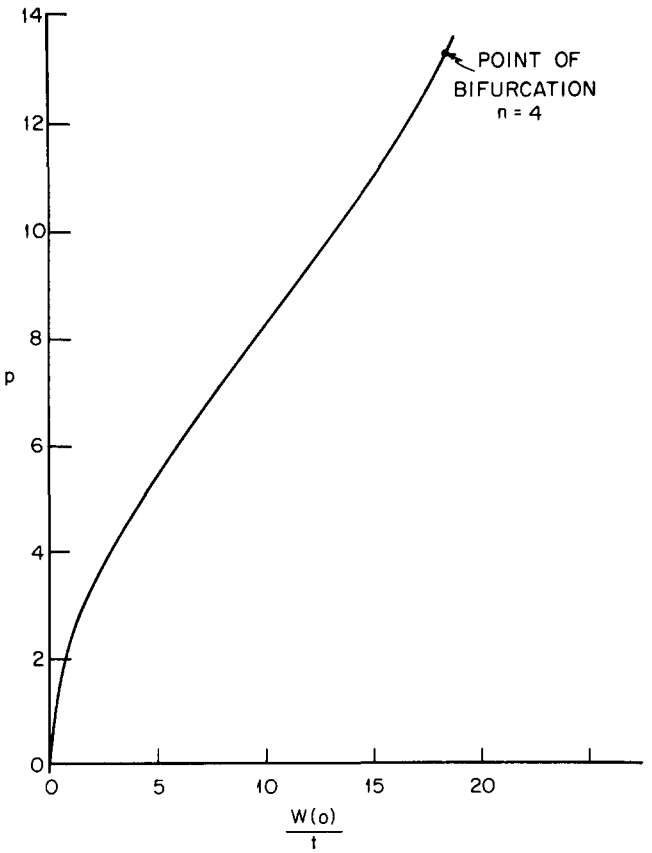

FIG. 7. Axisymmetric load–apex deflection curve $\lambda = 11$.

A, B and C are 2×2 coefficient matrices, and d is a two-component vector. The boundary conditions (B4)–(B6) lead to the equations

$$-G\delta y_{N-1} + H\delta y_N + G\delta y_{N+1} = 0 \tag{B8}$$

$$\delta y_1 = 0 \tag{B9}$$

where G and H are again 2×2 matrices and an $(N+1)$st mesh point has been introduced to permit a central difference representation of derivatives on the boundary $x = \lambda$. The system of equations was completed by applying (B7) at $j = N$. The solution of the system was effected by Potters' method [17]. In the application of this method a vector s_j and a matrix Q_j are introduced by writing

$$\delta y_j = s_j + Q_j \delta y_{j+1}, \qquad j = 1, 2, \ldots, N \tag{B10}$$

Substitution in (B7) leads to the recurrence relations

$$\begin{aligned} s_j &= (A_j Q_{j-1} + B_j)^{-1}(d_j - A_j s_{j-1}) \\ Q_j &= -(A_j Q_{j-1} + B_j)^{-1} C_j \\ j &= 2, 3, \ldots, N . \end{aligned} \tag{B11}$$

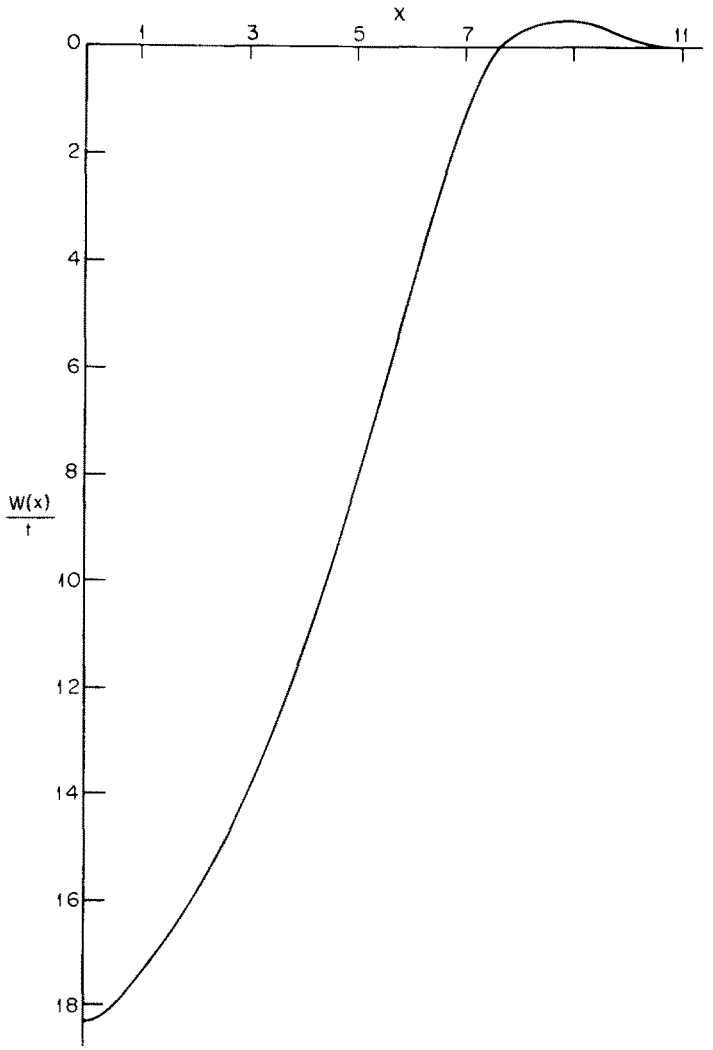

FIG. 8. Axisymmetric vertical deflection $\lambda = 11$ $p = p_c = 13{\cdot}28$.

Equation (B11) is applied at $j = 2$ by taking

$$s_1 = 0; \qquad Q_1 = 0\,. \tag{B12}$$

Finally, by combining (B8) and the result of applying (B7) at $j = N$, one obtains

$$\delta y_{N+1} = [G + HQ_N - GQ_{N-1}Q_N]^{-1}[G(s_{N-1} + Q_{N-1}s_N) - Hs_N]\,. \tag{B13}$$

The solution is now accomplished by sequential application of (B12), (B11), (B13) and (B10).

Buckling problem

With a procedure available for finding the axisymmetric solution at a given load the buckling loads can be calculated. Potters' method was again employed. This method has

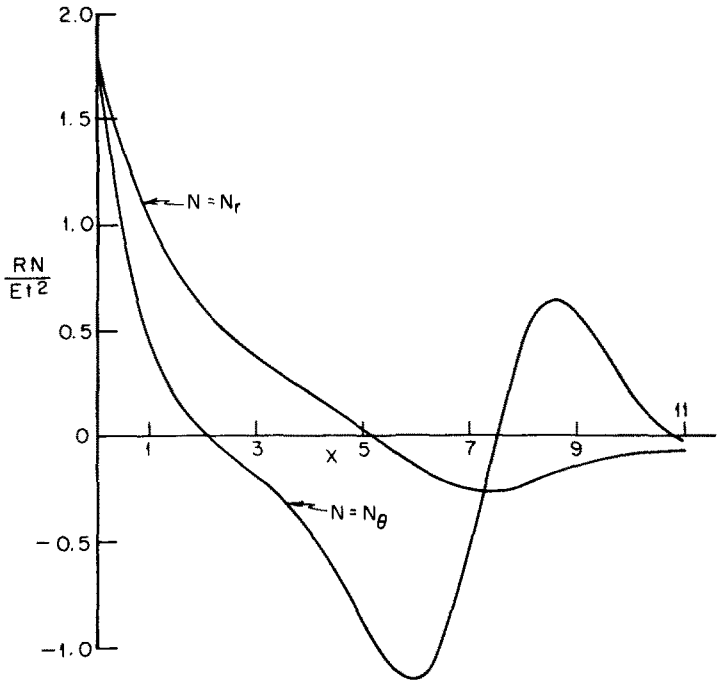

FIG. 9. Axisymmetric radial and tangential stress resultants $\lambda = 11$ $p = p_c = 13{\cdot}28$.

previously been applied to equations (13)–(18) by Huang [12] for the uniform pressure case. Again dividing the shell meridian as before and using central difference formulas (13) and (14) can be written in the matrix form

$$A_j y_{j-1} + B_j y_j + C_j y_{j+1} = 0, \qquad j = 2, 3, \ldots, N-1 \tag{B14}$$

where A, B, and C now represent 4×4 matrices some of whose elements involve the solution of the axisymmetric problem and

$$y = \begin{Bmatrix} w_{1n} \\ f_{1n} \\ w''_{1n} \\ f''_{1n} \end{Bmatrix}.$$

The boundary conditions (15)–(18) take the form

$$-Gy_{N-1} + Hy_N + Gy_{N+1} = 0 \tag{B15}$$

where G and H are also 4×4. It is readily shown that the apex conditions (19) are equivalent to the statement $A_2 y_1 = 0$. Again the system is completed by application of (B14) at $j = N$. Since the system is homogeneous one now writes

$$y_j = Q_j y_{j+1}, \qquad j = 1, 2, \ldots, N \tag{B16}$$

which leads to the recurrence relation

$$Q_j = -(A_j Q_{j-1} + B_j)^{-1} C_j, \qquad j = 2, 3, \ldots, N \tag{B17}$$

with $Q_1 = 0$. Equations (B14) (at $j = N$) and (B15) may be combined to obtain

$$(G+HQ_N-GQ_{N-1}Q_N)y_{N+1} = 0\,.$$

The condition for a non-trivial solution thus becomes

$$|G(I-Q_{N-1}Q_N)+HQ_N| \equiv |S| = 0 \tag{B18}$$

where I denotes the identity matrix. The zeros of $|S|$ were located by calculating its value for each of a closely spaced sequence of load values. A recent paper by Blum and Fulton [21] proved extremely helpful in carrying out this procedure. These authors show that, in addition to zeros, this determinant is likely to have singular points at which it also changes sign. The presence of such points can lead to obvious practical difficulties in locating the zeros. They suggest a "fix" which removes the sign changes associated with the singularities. Their procedure is based on recognition of the fact that the full determinant of the linear system (B14, 15) can be written in the form

$$D(p) = |B_2|\,.\,|B_3+A_3Q_2|\,.\,|B_4+A_4Q_3|\ldots|B_N+A_NQ_{N-1}|\,.\,|S|\,. \tag{B19}$$

Now, assuming that D itself is a continuous function of the load, its only sign changes will be associated with its zeros. Thus, by computing

$$(\text{sign of } D)\,.\,(\text{absolute value of } |S|)$$

rather than $|S|$ itself, the sign changes associated with the singularities of $|S|$ are removed. The sign of D is found by determining the sign of each factor in (B19) at the time the corresponding matrix is inverted for use in (B17).

(*Received* 28 *April* 1967; *revised* 21 *August* 1967)

Абстракт—Исследуется упругое выпучивание и начальное поведение после выпучивания заделаных, пологих, сферических оболочек, нагруженных сосредоточенной силой. Определяется, что бифуркация несимметричной формы изгиба появится перед осесимметричном внезапным выпучиванием, несмотря на это, что отношение высоты оболочки к толщине находится в узком интервале, соответствующим относительного толстым оболочкам. Начальный анализ поведения после выпучивания указывает, что оболочка сохраняет свою несущую способность пра переходе к несимметричной форме выпучивания. Эти результаты являются, качественно согласными, с доступными экспериментальными результатами.